A versatile chemical method for the formation of macroporous transition metal alloys from cyanometalate coordination polymers†

Christine M. Burgess, Martina Vondrova and Andrew B. Bocarsly*

A facile two-step synthetic route to macroporous metal and metal alloy frameworks from hydrogel-forming coordination polymers known as cyanogels is described. The polymerization of a chlorometalate and cyanometalate in aqueous solution results in the formation of a cyanogel that will auto-reduce at elevated temperatures to form metal alloys under an inert atmosphere. Cyanogels are versatile precursors to macroporous metals due to the large number of metal alloy systems that can be produced. This synthetic route is advantageous due to the production of uncontaminated final products of refractory metals at low temperatures. Transient reactive liquid sintering is shown to be the physical process through which macroporous metal forms from the cyanogel precursor.

Introduction

Macroporous metals possess interesting combinations of properties such as high gas permeability coupled with high thermal conductivity, which make them amenable to a diverse range of applications including heterogeneous catalysis, electrochemistry, acoustic control and biofiltration.[1,2] Specifically, macroporous frameworks of palladium and platinum alloys are attractive synthetic targets owing to the catalytic properties of these alloys.[3,4] Such porous materials have potential advantages in certain catalytic applications when compared to the small stabilized particles often used in heterogeneous catalysis. For example, macroporous metals have a relatively high surface area that is obtained without the need for stabilizing agents, which hinder the catalytic activity of small metal particles.[5,6] Another potential advantage of macroporous metals is the ability to produce porous monoliths from the catalytic material that will be robust at high temperatures and pressures.[7] The ability to produce porous metal monoliths would also greatly aid in catalysis recovery.

Historically, the synthesis of macroporous cellular metals has been approached through the direct mechanical manipulation of metallic melts; a successful strategy in particular for metals with low melting points, such as aluminium.[2,8,9] Easy access to the liquid state, afforded by a low melting point, is essential for processing techniques such as metal foaming or replication processing.[2,8–10] However, the synthesis of porous refractory metals, such as palladium and platinum, is not practical using such methods since the liquid state is hard to access and maintain.[9] Solid metal based techniques that rely on high processing temperatures and pressures or the incorporation of an additive, such as silicon have been developed to produce the desired metal morphology, but these approaches are complex and difficult to implement.[1]

Frick Laboratory, Department of Chemistry, Princeton University, Princeton, New Jersey 08544. E-mail: Bocarsly@princeton.edu
† Electronic supplementary information (ESI) available: Fig. S1–S4. See DOI: 10.1039/b804258f

Recently, several wet chemical methods based on the manipulation of solutions containing metal ions or nanoparticles as precursors have been developed for macroporous metal production.[11–14] However, the primary focus of such solution-based chemistry has been the synthesis of easily reducible gold and silver metal frameworks with limited work performed using alternative metals that do not offer the redox flexibility of the coinage metals.[11–13,15] Often, solution-based strategies are not amenable to alloy formation since alloying requires commensurate reduction kinetics and a high degree of spatial homogeneity, criteria that can be rarely achieved in reduction of soluble ions to the metallic state.[3,7]

We have previously reported that a sol–gel system, based on cyanide-containing coordination polymers, known as cyanogels, enables the facile synthesis of macroporous refractory alloys well below the melting point of the alloy.[21] The cyanogel precursor is an inorganic sol–gel formed through the reaction of aqueous solutions of a chlorometalate ($[MCl_4]^{2-}$, M = Pd, Pt) and a cyanometalate ($[M'(CN)_n]^{2-/3-}$, (n = 4,6; M' = Co, Pd, Fe, Ru, Os, Ni, Cr). This reaction results in the formation of an amorphous Prussian Blue-like polymer through the substitution of two *trans* chloride ligands on the chlorometalate by the nitrogen of the cyanometalate complex.[16] Polymerization results in the formation of a hydrogel with alkali chloride salts produced as by-products.[16] The polymeric material, when heated under an inert atmosphere, converts to metal in a multi-step process due to the ability of the bridging cyanide ligand to act as a reducing agent at elevated temperatures.[17–20] The mechanism through which the cyanogel is converted to bulk nonporous metal has previously been reported.[17] The auto-reduction of the Pd–Co system commences at approximately 220 °C. Reduction occurs concomitant with solid-state diffusion, which produces a homogeneous alloy due to the intimate mixing of the intermediate coordination compounds.[17] The redox properties of the cyanogel polymer, coupled with the homogeneous mixing of the different metals in the precursor, allow for the facile production of homogeneous alloys with tunable compositions as well as intermetallics.[21] Previously, we reported that thermal processing of a 500 mM 2 : 1 Pd–Co xerogel at 1000 °C for one hour,

reproducibly formed a macroporous Pd–Co alloy with a surface area of 5.16 m^2 g^{-1}.[18]

In this paper, we investigate the introduction of macroporosity in cyanogel-formed metal alloys. The mechanistic insight gained is used to generalize the reaction, allowing formation of a porous morphology for a wide variety of transition metal alloys and at significantly lower temperatures than originally observed in the Pd–Co system.

Experimental

Reagent grade Na$_2$PdCl$_4$ and K$_2$PtCl$_4$, were purchased from Pressure Chemical Company. K$_3$Co(CN)$_6$ and K$_2$Pd(CN)$_4$ were purchased from Aldrich while K$_4$Ru(CN)$_6$, was purchased from Alfa Aesar. All chemicals were used without further purification. The cyanoferrate starting materials, Na$_3$Fe(CN)$_5$NH$_3$ and Na$_3$Fe(CN)$_5$py (py = pyridine), were synthesized as previously described.[22,23]

Cyanogels incorporating [PdCl$_4$]$^{2-}$ were synthesized by mixing 500 mM aqueous solutions of chlorometalate and cyanometalate at room temperature. Cyanogels synthesized using [PtCl$_4$]$^{2-}$ were reacted at 90 °C to decrease gelation time. All hydrogels were aged at room temperature for one week in a closed container. Gels containing iron were reacted and aged under N$_2$ to prevent air oxidization of the iron and subsequent Prussian Blue formation. During aging, irreversible syneresis was observed in all cyanogel samples.[24] Gels synthesized with Pd–Co ratios less than 1.5 : 1 Pd–Co were reacted in the presence of 1 M NaCl. The hydrogel precursors must be aged for at least one week at room temperature for porous metal to be produced. After aging was complete, the water expelled during syneresis was removed through filtration and the resulting material was dried at 70 °C overnight to produce a xerogel.

In this report, the cyanogels will be denoted by the ratio of included components. For example, a cyanogel synthesized from mixing 500 mM aqueous solutions of Na$_2$PdCl$_4$ and K$_3$Co(CN)$_6$ in a 2 to 1 volumetric ratio will be referred to as a 2 : 1 Pd–Co cyanogel. For simplicity, when a cyanide ligand is replaced by another ligand, the replacement ligand will be referred to as a subscript to the metal (for example, Na$_3$Fe(CN)$_5$NH$_3$ is referred to as Fe$_{NH_3}$).

In one set of experiments, the sodium and potassium chloride by-products of gelation were exchanged with CsCl (Aldrich) by first soaking a 2 : 1 Pd–Co hydrogel in a distilled water bath at 9 °C. The bath was changed daily until reacting an aliquot of the bath water with 0.12 M AgNO$_3$ (Alfa Aesar) produced no precipitate, indicating that all unbound metal chloride salts had been leached from the gel. The washed hydrogel was then exposed to increasing concentrations of CsCl (from 0.1 M to 1.0 M) over a one week period. The xerogel of this material was produced as described above.

Reduction to metal was achieved by heating the xerogel material in a flowing argon atmosphere (60 mL min^{-1}) using a 3-zone programmable 2416-cm^3 Carbolite furnace or a Perkin–Elmer thermogravimetric analyzer (TGA-7). Unless otherwise noted, samples were heated to 1000 °C at a ramp rate of 12 °C per min and held for one hour at that temperature. Zirconium metal (Alfa Aesar) was used as an O$_2$ scavenger. At least five samples were thermally processed to confirm that the observed

morphology was reproducibly generated. **Warning**: *By-products of the thermal processing are hydrogen cyanide and cyanogen. These gases must be trapped by bubbling the furnace exhaust through a solution of bleach followed by a 1.0 M aqueous NaOH solution.*

X-Ray powder diffraction (XRD) patterns were measured on a Rigaku Minifex using a Cu (Kα) source (1.5406 Å). Scanning electron microscopy (SEM) and energy dispersive X-ray spectroscopy (EDX) were performed using a FEI XL30 FEG-SEM equipped with a PGT-IMIX PTS EDX system utilizing an accelerating voltage of 15 KeV. Infrared spectra (IR) were measured on a Nicolet Model 720 FTIR spectrophotometer using KBr pellets. A HP 8453 diode array spectrophotometer was used to obtain UV-visible spectra.

Results and discussion

The 2 : 1 Pd–Co xerogel precursor to the previously reported macroporous Pd–Co alloy is a composite of an amorphous coordination polymer, NaCl and KCl.[18] The alkali chloride salts are a by-product of the polymerization process and are deposited throughout the coordination polymer as the solvent is removed from the hydrogel to produce the xerogel. Heating the xerogel to 1000 °C for 1 hour results in the formation of the desired macroporous Pd–Co alloy (Fig. 1a, Table 1). XRD and EDX analysis of the Pd–Co alloy show that it is a pure material with no alkali chloride by-products or other contaminants remaining (Table 1 and Fig. S1, see ESI†). The composition of the Pd–Co alloy can be altered by modifying the initial ratio of Pd to Co in the cyanogel precursor. (Table 1, Fig. S2, see ESI†).

A non-porous Pd–Co alloy is produced after heating to 1000 °C if the alkali chloride by-products of the polymerization process are removed prior to heating from a 2 : 1 Pd–Co xerogel through washing with water until no peaks for crystalline alkali chloride salts are seen in the XRD of the xerogel (Fig. 1b). Thus, while metal formation does not require the presence of an alkali chloride, macroporosity in the product is dependent on having alkali halide salt present in the xerogel phase.

Removal of the alkali chloride from the dehydrated xerogel material is an irreversible process. Soaking the alkali chloride-free Pd–Co xerogel in a 1.0 M aqueous NaCl solution for three hours does not regenerate the xerogel's ability to produce a porous material when heated to 1000 °C. Previous work on the cyanogel system has shown that removal of water from the hydrogel to produce the xerogel causes significant pore collapse due to the stresses involved in the drying process, a phenomenon common in sol–gel processing.[25] When the alkali chloride is present during the drying of the hydrogel, the alkali chloride is deposited throughout the xerogel. Pore collapse prevents the same deposition occurring when the alkali chloride-free Pd–Co xerogel is soaked in an alkali chloride solution; thus, the location of the alkali chloride in the precursor is a crucial factor in the formation of porous metal products.

At a working temperature of 1000 °C, the mixture of KCl and NaCl present in the precursor is expected to be a liquid[26] that will evaporate into the flowing stream of argon present in the furnace runs. The expected evaporation of the halide salts is observed to occur in TGA experiments.[18] Alkali chloride evaporation is found to be essential to the formation of the macroporous

This journal is © The Royal Society of Chemistry 2008

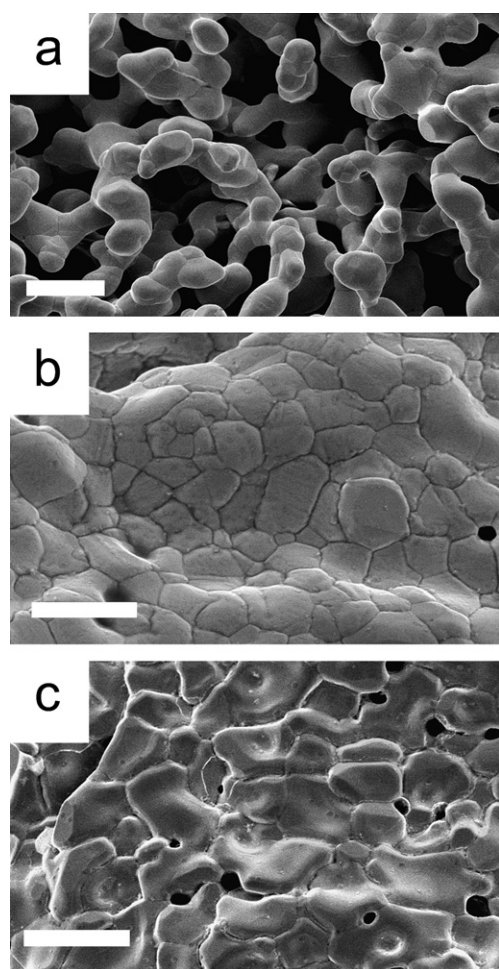*J. Mater. Chem.*, 2008, **18**, 3694–3701 | 3695

Fig. 1 Morphology of the Pd–Co alloy produced from heating a 2 : 1 Pd–Co xerogel to 1000 °C for one hour is determined by both the presence and thermal evaporation of the alkali chloride by-product of gel formation. a) Heating the native 2 : 1 Pd–Co system produces a macroporous framework. Scale bar represents 20 μm. b) Removing the alkali chloride from the 2 : 1 Pd–Co precursor prevents macroporous metal framework formation. Scale bar represents 10 μm. c) Preventing alkali chloride evaporation by heating the native precursor in a stagnant atmosphere also prevents the formation of a macroporous network. Scale bar represents 20 μm.

Table 1 Composition of metal produced by heating cyanogel precursors to 1000 °C for one hour. Compositions of alloys were calculated from XRD data by using linear interpolation between the lattice parameters of the pure metals ($a_{Pd} = 3.8874$ Å, $a_{Fe} = 3.6544$ Å, $a_{Co} = 3.563$ Å and $a_{Pt} = 3.9242$ Å)[35] except for the Pd–Co system, which was determined by utilizing a calibration curve relating palladium content and palladium cobalt alloy lattice parameters.[36] Uncertainty of XRD compositions are based on the uncertainty of 0.1° in assigning the position of the peaks. Composition by EDX is based on 20 data points for each sample

Cyanogel precursor	Metal product (lattice parameter ±0.009)	Composition	
		XRD	EDX
2 : 1 Pd–Co	FCC Pd–Co alloy ($a = 3.821$ Å)	$77 \pm 3\%$ Pd	$75 \pm 4\%$ Pd
1.5 : 1 Pd–Co	FCC Pd–Co alloy ($a = 3.798$ Å)	$65 \pm 3\%$ Pd	$67 \pm 3\%$ Pd
1 : 1 Pd–Co (1 M NaCl)	FCC Pd–Co alloy ($a = 3.751$ Å)	$50 \pm 3\%$ Pd	$53 \pm 4\%$ Pd
2 : 1 Pd–Pd	FCC Pd metal ($a = 3.887$ Å)	FCC Pd	100% Pd
2 : 1 Pd–Ru	FCC Pd metal ($a = 3.885$ Å)	FCC Pd	$74 \pm 2\%$ Pd
	HCP Ru metal ($a = 2.706$ Å)	HCP Ru	
2 : 1 Pd–Fe$_{NH_3}$	FCC Pd–Fe alloy ($a = 3.861$ Å)	$95 \pm 3\%$ Pd	$94 \pm 2\%$ Pd
2 : 1 Pd–Fe$_{py}$	FCC Pd–Fe alloy ($a = 3.814$ Å)	$82 \pm 3\%$ Pd	$81 \pm 4\%$ Pd
2 : 1 Pt–Co	FCC Pt–Co alloy ($a = 3.824$ Å)	$75 \pm 3\%$ Pt	$73 \pm 3\%$ Pt

evaporation of the alkali chloride at high temperatures in the native system resulted in an average grain size of 15.3 ± 1.7 μm. All three grain sizes were found to be statistically different using a Student's t-test at the 99% confidence level.

Morphological changes due to removal of the alkali chloride or prevention of complete evaporation of the alkali chloride suggests that an interaction between alkali chloride and metal (not the polymeric precursor) is the key step in the production of a macroporous alloy from the cyanogel precursor. To confirm such an interaction, the thermal treatment of the cyanogel was halted after auto-reduction of the polymer was complete but before evaporation of the alkali chloride commenced. Reheating this intermediate allows for the high temperature metal–alkali chloride interaction to be probed directly. A 2 : 1 Pd–Co xerogel was heated to 650 °C for 1 hour under argon to produce the metal–alkali chloride intermediate, MS. The temperature, 650 °C, was chosen as previous work had shown complete auto-reduction of the 2 : 1 Pd–Co xerogel, but no loss of alkali halide, at this temperature.[18] Total auto-reduction of the polymer was confirmed in MS by IR which showed no cyanide stretches (Fig. 2). XRD of MS showed peaks for a FCC Pd–Co alloy, NaCl and KCl. (Fig. 3a) EDX analysis of the surface and fractured cross-sections of MS, showed signals for Pd, Co, Na, K and Cl, which were evenly distributed through out the material. (Fig. S3, ESI†) To image the metal framework, the alkali chloride salt was removed from MS by washing with deionized water to produce metal M. SEM analysis revealed M to be a rough metallic material with limited void space (Fig. 4a). This morphology is in stark contrast to that of the metal produced from the same xerogel when heated to 1000 °C (Fig. 1a). This morphological difference is an indication that the alkali chloride
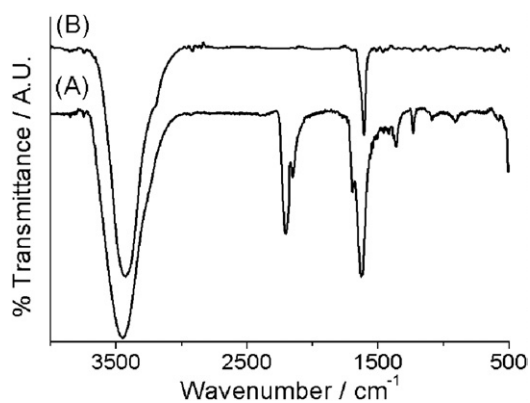
product. If a 2 : 1 Pd–Co xerogel is heated to 1000 °C for 1 hour under a stagnant argon atmosphere, porosity does not develop in the product (Fig. 1c). XRD analysis of the resulting metal shows the presence of the Pd–Co alloy, along with NaCl and KCl indicating that alkali chloride evaporation is limited in the absence of a flowing gas stream. Thus, the extended interaction between metal and alkali chloride at high temperatures appears detrimental to macroporous metal formation.

Morphological differences resulting from changes in the alkali chloride interaction with the system are coupled with changes in the metal product grain size (Fig. 1). The amount of time that the metal interacts with the alkali chloride is proportional to the overall grain size of the final product. The average grain size of the metal produced from the alkali chloride-free Pd–Co xerogel was found to be 4.1 ± 0.97 μm. The average grain size for the native system was found to be 8.6 ± 3.3 μm, and preventing the

Fig. 2 Heating a 2 : 1 Pd–Co xerogel to 650 °C for one hour results in complete auto-reduction of the initial polymer. A) FTIR of starting material with characteristic bridging (2195 cm^{-1}) and terminal (2151 cm^{-1}) cyanide stretches associated with a Pd–Co xerogel. B) FTIR of the material after heating shows only peaks associated with water and no cyanide stretches indicating that complete auto-reduction to metal has occurred.
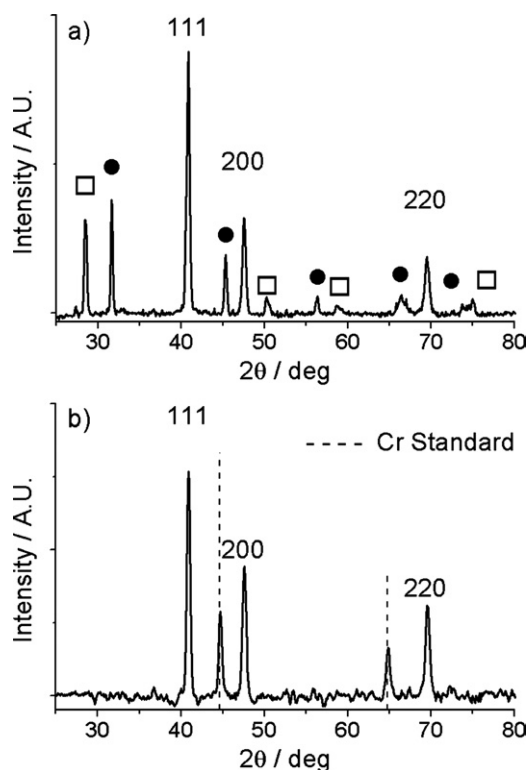

Fig. 3 High temperature heating results in evaporation of the alkali chloride by-products of polymerization with no change to Pd–Co alloy lattice parameter. a) Heating a 2 : 1 Pd–Co xerogel to 650 °C produces composite material MS, which is composed of an FCC Pd–Co alloy (lattice parameter (a) =3.821 Å), KCl (□) and NaCl (●). b) Heating MS to 1000 °C results in the complete removal of the alkali chloride salts with no change to the FCC Pd–Co lattice parameter (a = 3.821 Å). The vertical dashed line marks an internal chromium standard.

is not acting as a templating agent during the conversion of polymer to metal.

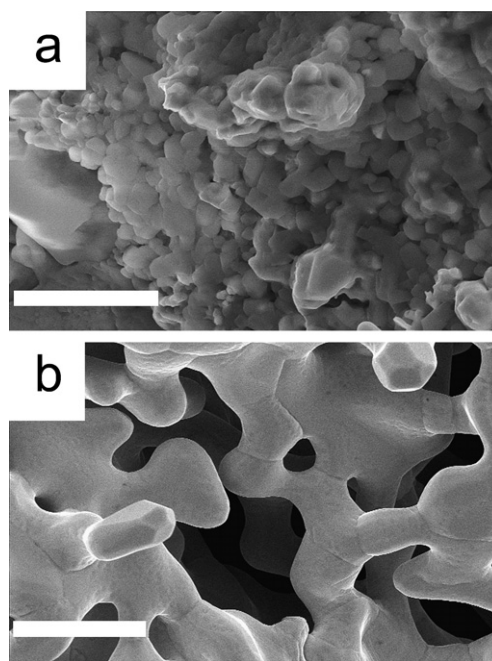X-Ray powder analysis and EDX analysis of the product formed by heating MS at 1000 °C for one hour showed that no

Fig. 4 Macroporous metal network formation is the result of a high temperature metal–alkali chloride interaction. a) SEM showing morphology of metal in Pd–Co–alkali chloride adduct MS, which is produced by halting thermal treatment of the xerogel at 650 °C. b) SEM of the porous metal framework, which results from heating MS to 1000 °C. Note the drastic morphological change that occurred on heating MS to high temperature. Scale bars represent 20 μm.

alkali chloride salt remained in the material (Fig. 3b). SEM analysis of the final product showed a drastic morphological change in the metal material when MS was reheated (Fig. 4), signifying that a high temperature interaction (>650 °C) between metal and alkali chloride induces the spongy morphology. In contrast, heating alkali chloride-free M to 1000 °C did not result in a morphological change in the metal. The lattice parameter of the Pd–Co alloy in MS does not change upon reheating to 1000 °C, which indicates that preferential leaching of one of the metal components of the alloy does not play a significant role in the formation of the macroporous material (Fig. 3).

Fluxes formed from molten alkali chloride salts are known to oxidize transition metals to their respected metal chlorides.[27] The solubility of the Pd–Co alloy of interest in a sodium/potassium chloride flux was confirmed by heating a Pd–Co alloy synthesized from a cyanogel precursor in the presence of an excess of NaCl and KCl to 1000 °C for 1 hour. This halide system is reported to form an eutectic that melts at 665 °C.[26] A large excess of alkali chloride was used to prevent complete evaporation of the alkali chloride before the sample could be evaluated. When removed from the furnace, the remaining alkali chloride had a bright blue color suggesting that $CoCl_2$ was present. The existence of $CoCl_2$ was confirmed by extracting the alkali chloride with acetone and subsequent analyses of the acetone solution using UV-visible spectroscopy (Fig. S4, ESI†). The acetone extract showed peaks at λ_{max} = 674 nm and 636 nm, which are associated with Co^{2+} complexes of acetone and Cl^-.[28] UV-visible spectroscopy of the remaining alkali chloride dissolved in water showed peaks at λ_{max} = 279 nm and 222 nm that corresponds to $PdCl_4^{2-}$.[29]

This evidence collectively suggests that a transient reactive liquid-sintering process is behind the formation of macroporous metal from a cyanogel precursor. The first step in transient reactive liquid sintering involves the dissolution of the solid into the reactive liquid.[30,31] In the cyanogel system, solubility occurs through oxidation of the initial non-porous metallic intermediate, resulting in the formation of soluble metal chloride complexes.[27] It is expected that oxidation of the initially formed nonporous metallic species by the alkali halide flux is an equilibrium process based on the known behavior of high temperature halide fluxes.[27] The equilibrium constant for this process should be higher in regions of the metal with higher surface energy.[30,31] Spatial differences in the redox equilibrium constant is expected to result in the effective movement of zero-valent metal from areas of high surface energy, such as the edges of small particles, to areas of lower surface energy, such as well-developed crystalline faces.[30,31] Metal grain growth should result from exposure of the metallic intermediate to the alkali chloride melt, and is expected to increase as the contact time with the alkali chloride flux increases, as was experimentally observed. The first expected product of a reactive liquid-sintering process is the formation of a porous network due to grain growth.[30,31] In the systems under investigation, this porous intermediate is trapped due to the evaporation of the alkali chloride flux in the flowing gas stream (Fig. 1a). When evaporation of the alkali chloride is limited the complete densification of the substrate is observed, the expected final step in reactive liquid sintering (Fig. 1c).[30,31]

Reduction of working temperature through alkali chloride replacement

Given the mechanism elucidated in the prior section, it is expected that spongy morphologies can be achieved at a lower temperature by introducing an alkali chloride with a lower melting point into the cyanogel. To test this concept, the alkali chloride by-product in the Pd–Co system was replaced with CsCl, which has a melting point of 649 °C.[26,32] Alkali chloride exchange was achieved by first soaking a 2 : 1 Pd–Co hydrogel in distilled water to remove all non-bound salt. The sample was subsequently exposed to solutions of increasing CsCl concentration to ion exchange out any bound sodium and potassium ions as well as produce an excess of CsCl in the gel. Once the hydrogel was impregnated with CsCl it was dried to produce the xerogel. Salt replacement was confirmed by XRD of the xerogel, which showed CsCl as the only crystalline phase (Fig. 5a). IR analysis of the CsCl xerogel showed a shift in the terminal cyanide stretch from 2151 cm^{-1}, found in the native xerogel, to 2130 cm^{-1} (Fig. 5b). Previous work has shown that terminal ν_{CN} stretches are sensitive to changes in cation identity.[33] Based on this data, it was concluded that CsCl was present throughout the xerogel material and not just as a surface layer. Heating the CsCl xerogel at 655 °C for 12 hours produced the macroporous framework shown in Fig. 6. Heat treatment of a native xerogel at 655 °C for 12 hours did not produce a porous framework. The ability to produce a macroporous metal at a lower temperature through lowering the melting point of the alkali chloride further supports a transient reactive liquid-sintering process.

The porous network generated using a CsCl flux has smaller pore diameters and metal framework widths (defined as the
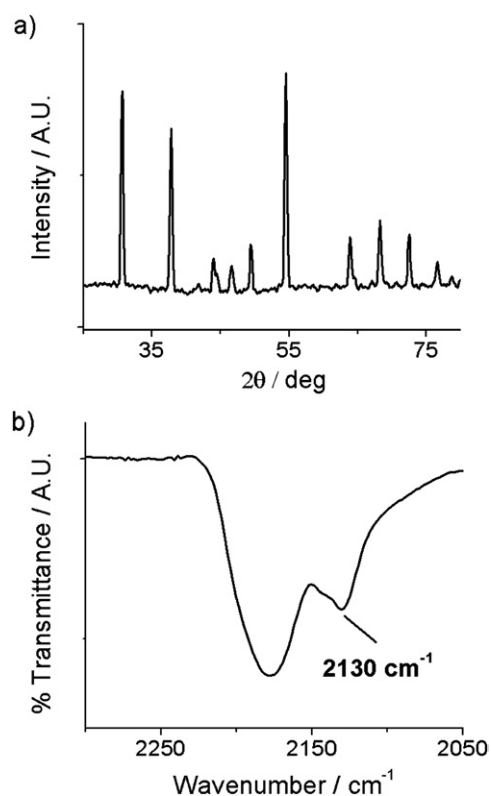

Fig. 5 Exposing a salt-free 2 : 1 Pd–Co hydrogel to aqueous solutions of CsCl allows for the impregnation of CsCl throughout the gel. a) XRD analysis of the xerogel produced from the CsCl exposed hydrogel shows CsCl as the only crystalline material in the xerogel. b) IR analysis shows a shift of the terminal cyanide stretch to 2130 cm^{-1} indicating a change in counter-ion.
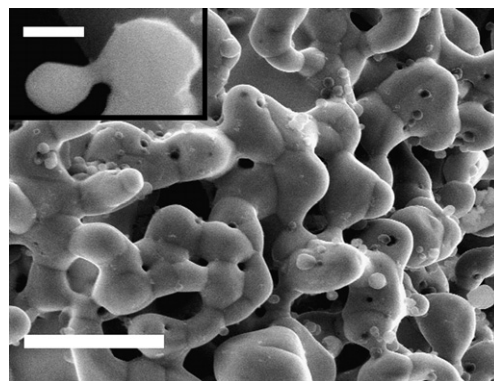

Fig. 6 Changing the alkali chloride present in the precursor xerogel significantly reduces the temperature necessary to produce a macroporous framework. SEM image of the macroporous metal produced from a heated CsCl xerogel at 655 °C for 12 h. Scale bar represents 5 μm. Insert shows one of the sinter necks present in the material, scale bar represents 500 nm.

shortest distance between two void spaces), than the native system (Table 2). In contrast to the NaCl/KCl system, small particles of metal were seen in the CsCl-treated material with sinter necks attaching the particles to the main network (Fig. 6 insert), suggesting that sintering occurs at a slower rate in the

Table 2 Average pore diameters and network widths of the macroporous metal products with standard deviation using at least 50 measurements per sample

Metal system	Average pore diameters/μm	Average network width/μm
Pd–Co alloy (native system)	6.5 ± 4.3	7.0 ± 2.1
Pd–Co alloy (CsCl system)	1.9 ± 1.3	1.7 ± 0.5
Pd–Ru composite	1.7 ± 0.5	1.3 ± 0.4
Pd metal	5.7 ± 3.9	8.3 ± 1.4
Pd–Fe alloy	4.5 ± 3.2	4.2 ± 0.9
Pt–Co alloy	3.1 ± 2.7	2.9 ± 1.3

CsCl system than in the original system. The decreased sintering rate may be attributed to either decreased ion mobility in the CsCl melt or a decreased solubility of the Pd–Co alloy in the melt. Both decreased ion mobility and lower solubility are expected due to the lower processing temperature used and the reduced oxidizing power of Cs^+ in comparison with Na^+ or K^+.[34] Changes in pore size and network width suggests that control over final morphology can be gained through alterations in the alkali chloride flux used.
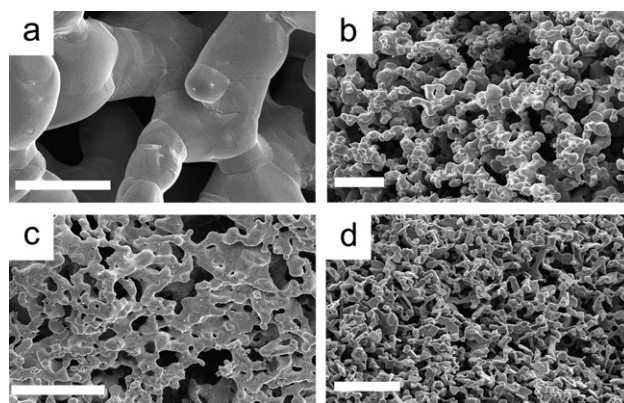
Extension to other alloys, metals and composite systems

The observation of a transient reactive liquid-sintering mechanism in the Pd–Co system suggests that the formation of macroporous metal frameworks should be a general phenomenon of cyanogel systems as all cyanogel coordination polymers produce alkali chloride by-products in the polymerization process. To test the general nature of this synthetic approach, 2 : 1 Pd–Fe$_{NH_3}$, Pd–Fe$_{py}$, Pd–Pd, Pd–Ru, and Pt–Co xerogels were synthesized and characterized using IR (Table 3). In all samples, the frequency of the carbon nitrogen stretch (ν_{CN}) shifted to higher wavenumbers than in the monometallic cyanometalate precursor, indicating that polymerization had occurred through the formation of bridging cyanide ligands (Table 3).

Heating the xerogel precursors to 1000 °C for one hour under flowing argon resulted in the formation of macroporous metals in all cases (Fig. 7). The average width of the metal network and the average size of the pores were estimated for all systems from SEM data (Table 2). The structure of the macroporous metal network produced from both of the ligand-substituted

Fig. 7 The formation of macroporous metal using cyanogel precursors is a general technique due to the nature of transient liquid sintering. SEM micrographs of metals produced through heat treatment of various xerogels at 1000 °C for 1 hour: a) palladium metal, 10 μm scale; b) platinum cobalt alloy, 20 μm scale; c) palladium iron alloy, 20 μm scale; d) palladium ruthenium composite, 10 μm scale.

pentacyano iron systems was found to be identical through SEM analysis. With the exception of the Pd–Fe systems, the morphology of the metal was found to be extremely consistent throughout each sample. In the Pd–Fe systems, several regions of crystalline stairs were seen where it appeared that the network had sintered together (Fig. 8).

The compositions of the metal frameworks were determined using XRD and EDX (Table 1). In all cases, the compositions calculated from XRD were in good agreement with EDX analysis. Both EDX and XRD analysis showed that the metal was the only material found in the final product. This is in agreement with previous analysis that has shown the metal produced from cyanogels is of high purity.[21] EDX mapping of the Pd–Ru composite material (Fig. 9) did not show any observable separation between the two metals, indicating that the two are intimately mixed on a length scale of less then 1 μm, which is the resolution of the EDX system used.

A transient reactive liquid-sintering mechanism explains the variations in morphology with transition metal composition that are observed (Fig. 7). The solubility of the metal in the halide flux is related to the ability of the salt to oxidize the metal.[27] The free energy needed to oxidize the metals used in this study increases in the following order:[34]

Table 3 Cyanide stretching frequency (ν_{CN}) of xerogels and corresponding cyano precursors showing that polymerization occurred through the formation of bridging cyanides during the gelation process
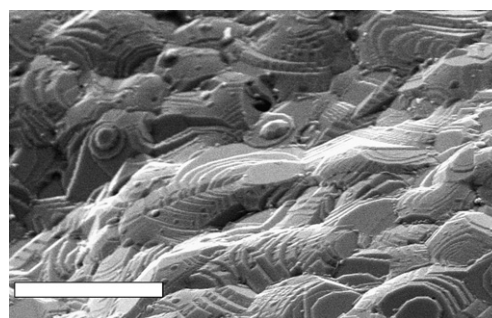
Cyanogel	Hydrogel color	ν_{CN} of cyanoprecursor/cm^{-1}	ν_{CN} of xerogel/cm^{-1}
2 : 1 Pd–Pd	Yellowish orange	2134	2210
2 : 1 Pd–Ru	Reddish orange	2042, 2027	2184, 2090
2 : 1 Pd–Fe$_{NH_3}$	Yellow	2088, 2048, 2036, 2013	2220, 2150
2 : 1 Pd–Fe$_{py}$	Dark orange	2090, 2047	2218, 2173, 2082
2 : 1 Pt–Co	Yellow	2126	2203, 2144

Fig. 8 Regions of the Pd–Fe porous network sinter together to form crystalline stairs in a small percentage of the sample. Scale bar represents 5 μm.
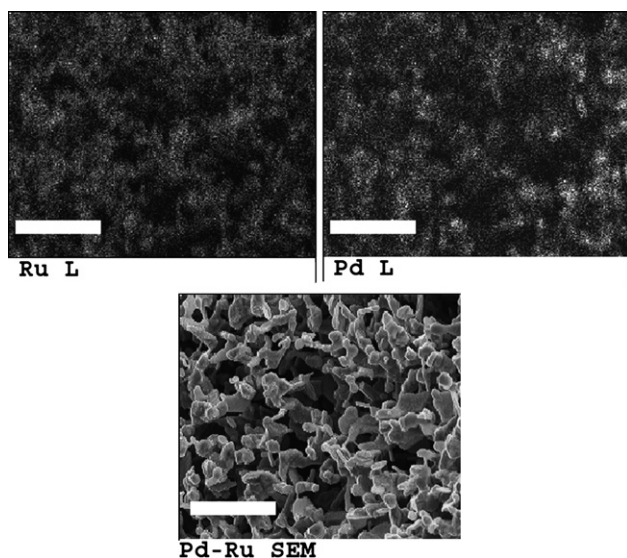
This journal is © The Royal Society of Chemistry 2008

J. Mater. Chem., 2008, **18**, 3694–3701 | 3699

Fig. 9 EDX map of Ru–Pd composite material showing that Ru and Pd are intimately mixed in the composite. Scale bars represent 5 μm.

$$Fe < Co < Ru < Pd < Pt$$

The platinum cobalt alloy has a network width that is significantly smaller than the palladium cobalt system (Fig. 7, Table 2). This is anticipated as the solubility of Pt metal is expected to be lower than the solubility of Pd based on the redox potential of the metal. This lower solubility would result in slower grain growth, which would in turn result in a smaller network given the same reaction time. The palladium iron system was the only one in which densification of the final material occurred in regions when the xerogel was processed in a flowing atmosphere (Fig. 8). Of the metals employed, iron is the most susceptible to corrosion in the molten salt environment. This increases the rate of sintering in the iron system, and therefore, decreases the time needed for complete densification to occur.

Conclusion

Cyanogels provide a simple "one-pot", two-step process for the production of macroporous transition metal alloys. This is significant given that a low-temperature technique for the facile production of macroporous palladium and platinum alloys has not been reported previously. Macroporosity is obtained by balancing the rate of reactive liquid sintering induced by the presence of an indigenous halide flux with the rate of flux removal by evaporation. The details of the process that generates the desired porosity can be controlled either by selection of the flux species *via* an ion-exchange process, or by regulations of the inert furnace atmosphere flow field.

Macroporous palladium and platinum alloys have potential applications in several fields including catalysis and as electrode materials where an enhanced boundary layer between a catalytic metal phase and a dissolved substrate is critical to productive reactivity. While many of the common synthetic routes to macroporous metals produce contaminated end products either as a by-product of the synthetic procedure or due to the necessity

of adding stabilizing agents such as small ceramic particles, the approach reported here produces a metal alloy free of contamination.[1,2,15,21] This is a particular strength of the processing technique reported here, since the presence of other materials in the final metal product affects properties such as catalytic behavior and mechanical strength.[1,2]

References

1 J. Banhart, *Prog. Mater. Sci.*, 2001, **46**, 559–U553.
2 H. Degischer and B. Kriszt, *Handbook of Cellular Metals: Production, Processing, Applications*, Wiley-VCH, Weinheim, 2002.
3 V. Ponec, G. C. Bond, *Catalysis by metals and alloys*, Elsevier Science, Amsterdam, 1995.
4 V. M. Schmidt, R. Ianniello, E. Pastor and S. Gonzalez, *J. Phys. Chem.*, 1996, **100**, 17901–17908.
5 B. R. M. Andrea, *Polym. Adv. Technol.*, 2001, **12**, 96–106.
6 C. W. Welch and R. G. Compton, *Anal. Bioanal. Chem.*, 2006, **384**, 601–619.
7 C. Bartholomew and R. Farrauto, *Fundamentals of Industrial Catalytic Processes*, Wiley, Hoboken, 2nd edn, 2006.
8 J. Banhart, *Adv. Eng. Mater.*, 2006, **8**, 781–794.
9 Y. Conde, J. F. Despois, R. Goodall, A. Marmottant, L. Salvo, C. San Marchi and A. Mortensen, *Adv. Eng. Mater.*, 2006, **8**, 795–803.
10 C. Gaillard, U. Despois and A. Mortensen, *Mater. Sci. Eng., A*, 2004, **374**, 250–262.
11 R. H. Jin and J. J. Yuan, *J. Mater. Chem.*, 2005, **15**, 4513–4517.
12 D. Walsh, L. Arcelli, T. Ikoma, J. Tanaka and S. Mann, *Nat. Mater.*, 2003, **2**, 386–U385.
13 H. F. Zhang and A. I. Cooper, *J. Mater. Chem.*, 2005, **15**, 2157–2159.
14 F. C. Meldrum and R. Seshadri, *Chem. Commun.*, 2000, 29–30.
15 B. C. Tappan, M. H. Huynh, M. A. Hiskey, D. E. Chavez, E. P. Luther, J. T. Mang and S. F. Son, *J. Am. Chem. Soc.*, 2006, **128**, 6589–6594.
16 B. W. Pfennig, A. B. Bocarsly and R. K. Prudhomme, *J. Am. Chem. Soc.*, 1993, **115**, 2661–2665.
17 M. Vondrova, T. M. McQueen, C. M. Burgess, D. M. Ho and A. B. Bocarsly, *J. Am. Chem. Soc.*, 2008, **130**, 5563–5572.
18 M. Heibel, G. Kumar, C. Wyse, P. Bukovec and A. B. Bocarsly, *Chem. Mater.*, 1996, **8**, 1504–1511.
19 B. Folch, J. Larionova, Y. Guari, L. Datas and C. Guerin, *J. Mater. Chem.*, 2006, **16**, 4435–4442.
20 M. Rehbein, M. Epple and R. D. Fischer, *Solid State Sci.*, 2000, **2**, 473–488.
21 M. Vondrova, C. M. Burgess and A. B. Bocarsly, *Chem. Mater.*, 2007, **19**, 2203–2212.
22 H. E. Toma and J. M. Malin, *Inorg. Chem.*, 1973, **12**, 2080–2083.
23 G. Brauer, *Handbook of Preparative Inorganic Chemistry*, Academic Press, New York, 1963.
24 J. L. Willson, *Ph.D. Thesis*, Princeton University, 2001.
25 R. S. Deshpande, S. L. Sharp-Goldman, J. L. Willson and A. B. Bocarsly, *Chem. Mater.*, 2003, **15**, 4239–4246.
26 L. Liu, W. A. Bassett and M. S. Liu, *J. Phys. Chem.*, 1973, **77**, 1695–1699.
27 *Corrosion*, ed. L. Shreir, R. Jarman and G. Burstein, Butterworth–Heinemann, Oxford, 3rd edn, 1994.
28 G. Stanescu and A. Trutia, *J. Optoelectron. Adv. Mater.*, 2005, **7**, 1009–1015.
29 L. I. Elding and L. F. Olsson, *J. Phys. Chem.*, 1978, **82**, 69–74.
30 A. Eremenko, Y. Naidich and I. Lavrineno, *Liquid-Phase Sintering*, Consultants Bureau, New York, 1970.
31 R. German, *Liquid Phase Sintering*, Plenum Press, New York, 1985.
32 *The Merck Index*, ed. M. O'Neil, Merck and Co., Whitehouse Station, 13th edn, 2001.

33 J. F. Bertran, J. B. Pascual and E. R. Ruiz, *Spectrochim. Acta, Part A*, 1990, **46**, 685–689.

34 D. Harris, *Quantitative Chemical Analysis*, W. H. Freeman and Company, New York, 6th edn, 2003.

35 *Pearson's Handbook of Crystallographic Data for Intermetallic Phases*, ed. P. Villars and L. D. Calvert, ASM International, Materials Park, Ohio, 2nd edn, 1991.

36 Y. Matsuo, *J. Phys. Soc. Jpn.*, 1972, **32**, 972.

This journal is © The Royal Society of Chemistry 2008

J. Mater. Chem., 2008, **18**, 3694–3701 | 3701